Publication IV

Lassi Karvonen, Songhak Yoon, Paul Hug, Hisao Yamauchi, Anke Weidenkaff, and Maarit Karppinen. 2011. The $n = 3$ member of the $SrCoO_{(3n-1)/n}$ series of layered oxygen-defect perovskites. Materials Research Bulletin, volume 46, number 9, pages 1340-1345.

Materials Research Bulletin 46 (2011) 1340–1345

Contents lists available at ScienceDirect

Materials Research Bulletin

journal homepage: www.elsevier.com/locate/matresbu

The $n = 3$ member of the $SrCoO_{(3n-1)/n}$ series of layered oxygen-defect perovskites

Lassi Karvonen [a,b], Songhak Yoon [b], Paul Hug [b], Hisao Yamauchi [a], Anke Weidenkaff [b], Maarit Karppinen [a,*]

[a] Laboratory of Inorganic Chemistry, Department of Chemistry, School of Chemical Technology, Aalto University, FI-00076 AALTO, Finland
[b] Laboratory for Solid-State Chemistry and Catalysis, EMPA - Swiss Federal Laboratories for Materials Science and Technology, CH-8600 Dübendorf, Switzerland

ARTICLE INFO

Article history:
Received 18 April 2011
Received in revised form 13 May 2011
Accepted 18 May 2011
Available online 26 May 2011

Keywords:
A. Oxides
B. Intercalation reactions
C. Thermogravimetric analysis
C. X-ray diffraction
D. Crystal structure

ABSTRACT

Topotactic oxygen deintercalation from cubic perovskite oxide $SrCoO_{3-\delta}$ ($\delta < 0.25$) is realized in a controlled way at low temperatures. Annealing in air at $200 < T < 275$ °C results in a three-phase region within $0.25 < \delta < 0.50$. Two of the phases are known previously, namely $SrCoO_{2.5}$, a phase with an orthorhombic brownmillerite-type (BM) structure, and $SrCoO_{2.75}$ (T1), a phase with a slight tetragonal distortion from cubic symmetry. The third phase (T2) has a strong tetragonal distortion, and appears to be the missing $n = 3$ member of the $SrCoO_{(3n-1)/n}$ series. Once the overall oxygen content reaches the value of $(3-\delta)_{aver} = 2.68(1)$, the T1-to-T2 phase conversion proceeds at constant $(3-\delta)_{aver}$. A more pronounced evolution of the c_{T2} lattice parameter as compared to the a_{T2} parameter implies a layered oxygen-vacancy-ordered structure for T2 with some flexibility for oxygen-content variation, in the style of the BM phase.

1. Introduction

Various chemical and electrochemical routes of topotactic oxygen intercalation/deintercalation have been successfully employed to produce new oxygen-vacancy-ordered structures out of late 3*d* transition metal oxides. In such reactions the cation lattice is typically left intact (excluding minor distortions). Topotactic reactions also often occur at low temperatures and – in many cases – the newly yielded structure is rather found to be destabilized upon heating even at moderate temperatures (100–300 °C). Two of the most well-known oxide systems allowing low-temperature topotactic oxidation/reduction are (i) the Ruddlesden-Popper oxides such as $La_2CoO_{4+\delta}$ [1], $La_2NiO_{4+\delta}$ [2] and $La_2CuO_{4+\delta}$ [3], and (ii) the perovskite oxides such as $SrFeO_{3-\delta}$ [4,5] and $SrCoO_{3-\delta}$ [6–11], the former accommodating the intercalated oxygen at interstitial sites and the latter at oxygen-vacancy sites. Examples of other structure types for which topotactic intercalation/deintercalation of oxygen through chemical and/or electrochemical reactions has been demonstrated are $YBaCo_4O_{7+\delta}$ [12], $CuYO_{2+\delta}$ [13] and $YBa_2Cu_3O_{7-\delta}$ [14].

The $SrCoO_{3-\delta}$ system has been known for its wide oxygen-deficiency range ($0.00 \le \delta \le 0.71$) including oxygen-ordered phases of orthorhombic [15,16], tetragonal [15] or cubic [6–8] symmetry. The orthorhombic $SrCoO_{2.50}$ ($\delta = 0.50$), which consists of alternating layers of corner-sharing CoO_4 tetrahedra and CoO_6 octahedra (as in the case of the mineral brownmillerite), is the most oxygen-deficient phase still exhibiting a long-range oxygen ordering [16]. The layered single-phase of the brownmillerite (BM) structure is flexible in terms of oxygen content within $0.48 < \delta < 0.58$. In the range of $0.58 < \delta < 0.71$ the structure is gradually reorganized into a 'mosaic' of brownmillerite-type nanodomains. The statistical distribution of domain orientations allows the low symmetry of crystallite domains to be observed only through local probing techniques, such as HRTEM and ED [17]. Instead, the spatially more averaging techniques, such as X-ray diffraction, erroneously conclude a cubic symmetry for $SrCoO_{2.29}$ ($\delta = 0.71$) [15,18]. On the other hand, intercalation of oxygen into the $SrCoO_{2.50}$ ($\delta = 0.50$, $n = 2$) phase turns the brownmillerite to the cubic $SrCoO_{3.00}$ ($\delta = 0.00$, $n = \infty$) phase *via* a cascade of tetragonally distorted oxygen-ordered $SrCoO_{(3n-1)/n}$ phases with oxygen contents of $(3n-1)/n$ oxygen atoms *per* formula unit. In addition to the earlier reported $n = 4$, 5 and 8 phases in electrochemically [7,8] and high-pressure and high-temperature [15] oxygenated samples, we recently observed signatures of the $n = 6$ and 7 phases in our multi-phase samples of $SrCoO_{3-\delta}$ ($0.13 < \delta < 0.50$) prepared through chemical oxidation [10].

The present work continues our chase for additional members in the $SrCoO_{(3n-1)/n}$ series. As a sample preparation technique, such a simple approach as air-annealing at moderately low temperatures [7,15] was employed, through which we were able to

* Corresponding author at: Laboratory of Inorganic Chemistry, Department of Chemistry, Aalto University School of Chemical Technology, P.O. Box 16100, FI-00076 AALTO, Finland. Tel.: +358 9 470 2 2600; fax: +358 9 462 373.
E-mail address: maarit.karppinen@aalto.fi (M. Karppinen).

0025-5408/$ – see front matter © 2011 Elsevier Ltd. All rights reserved.
doi:10.1016/j.materresbull.2011.05.028

identify for the first time the $n = 3$ phase within a newly found three-phase region with $2.50 < \delta < 2.75$.

2. Experimental

2.1. Sample preparation

For a starting material for reduction experiments, oxygen-rich $SrCoO_{3-\delta}$ powder was prepared through an EDTA (ethylenediaminetetraacetic acid) complexation method from stoichiometric amounts of Co and $SrCO_3$. Cobalt-metal powder was first set under a layer of H_2O, on top of which concentrated HNO_3 was added until the metal powder dissolved completely. $SrCO_3$ powder was then added in a similar manner. The resultant metal nitrate solution was poured into an equal volume of concentrated ammonia solution of EDTA in 200 mol-% excess with respect to the total amount of metal ions. The solution was heated to dryness, the residual being burned and then calcined in air at 900 °C for 5 h. Finally, the calcined powder was pelletized and sintered in air at 980 °C for 55 h, followed by quenching to room temperature. The pellets consisting of the orthorhombic brownmillerite-type $SrCoO_{2.5}$ phase were then immersed into a solution of 0.6 M H_2O and 2.5 M Br_2 in CH_3CN at 25 °C for 72 h for oxygenation. Under the acidic immersion, pellets disintegrated into a fine powder, which was washed with acetone after separation from the immersion. The resultant $SrCoO_{3-\delta}$ precursor powder was dried in air flow at 25 °C.

Four reduced samples were eventually prepared through annealing 300 mg batches of the precursor in 1 atm stagnant air as follows: [Sample A] 200 °C, 18 h; [Sample B] 250 °C, 12 h; [Sample C] 250 °C, 18 h; [Sample D] 275 °C, 18 h. Sample preparations were performed in a thermobalance (Netzsch STA 409 CD) in order to facilitate simultaneous observation of the weight (or oxygen-content) reduction. At the end of each reduction program, no change in sample weight was observed anymore.

2.2. Oxygen-content analysis

The overall oxygen content *per* formula unit, $(3-\delta)_{aver}$, of the samples each consisting of up to three oxygen-ordered phases, was determined by thermogravimetric (TG) analysis. The thermobalance was coupled with a quadrupole mass spectrometer (Netzsch MS 403 C Aeolos), which allowed us to detect the composition of the gaseous decomposition products. A powder sample of ~100 mg was heated up to 980 °C at a rate 7.5 °C/min under a reducing atmosphere (5 vol-% H_2/He). Calculations were made according to the overall decomposition reaction: $Sr_{1-x}CoO_{3-\delta}$ (s) + x $SrCO_3$ (s) → SrO (s) + Co (s) + $(3-\delta)$ H_2O (g) + x CO_2 (g) taking into account the presence of a tiny $SrCO_3$ impurity (*cf.* Section 3). The $SrCO_3$ content was defined from the last weight-reduction step at about 900 °C, which was accompanied with CO_2 (g) generation detected through MS analysis.

2.3. Phase identification

X-ray diffraction (XRD) data were collected for the samples with a PANalytical X'Pert PRO MPD powder diffractometer. Patterns for the precursor and the four reduced samples were collected with Cu-$K_{\alpha 1}$ radiation (filtered with a Ge(1 1 1)-crystal monochromator). Phases of the multi-phase patterns were indexed with the software TREOR [19]. Further analysis for extracting the lattice parameters was done with the multi-phase Le Bail profile matching tool implemented to the software JANA2000 [20]. Effects of the degree of oxygen deintercalation (and temperature) on the crystal structure and phase composition were also in situ observed with Cu-$K_{\alpha 1,2}$ radiation (Cu-$K_{\alpha 2}$ line was stripped off from the data by means of a software HighScore Plus) and Anton Paar XRK-900 reaction chamber. The same temperature program as the one used in the preparation of Sample B was chosen for the in situ study.

3. Results

The XRD pattern of the freshly synthesized $SrCoO_{3-\delta}$ precursor powder presented a single-phase cubic perovskite (see Fig. 1). However, long storage even at room temperature air ambient results in a small amount of $SrCO_3$ impurity phase, as is apparent in both the XRD and TG-MS data. As no X-ray reflections for cobalt-containing impurities were detected, it was understood that a slight A-site cation vacancy formation, typical for the perovskite compounds [21,22], takes place in the $Sr_{1-x}CoO_{3-\delta}$ lattice. Thermogravimetric analysis revealed a $Sr_{0.97(1)}CoO_{2.92(1)}$ stoichiometry for the precursor powder which had aged for 9 months before being used in this study. Apart from the minor $SrCO_3$ impurity, all the X-ray reflections detected for the precursor powder were readily indexed in $pm\bar{3}m$ space group with $a = 3.832(1)$ Å. Nearly identical values of $1-x = 0.97(1)$ for the A-site stoichiometry were also gained for the air-annealed samples (see Table 1).

In situ XRD observation of the pseudo-cubic perovskite $(1\ 1\ 1)_C$ reflection upon reductive annealing in air at 250 °C (Fig. 2(a), lower panel) reveals – as expected – a negative 2θ shift of the reflection indicating lattice expansion due to oxygen loss. Judging from the peak shift, the oxygen deintercalation continues for ca. 10 h, then the overall oxygen content $(3-\delta)_{aver}$ saturates. This is in

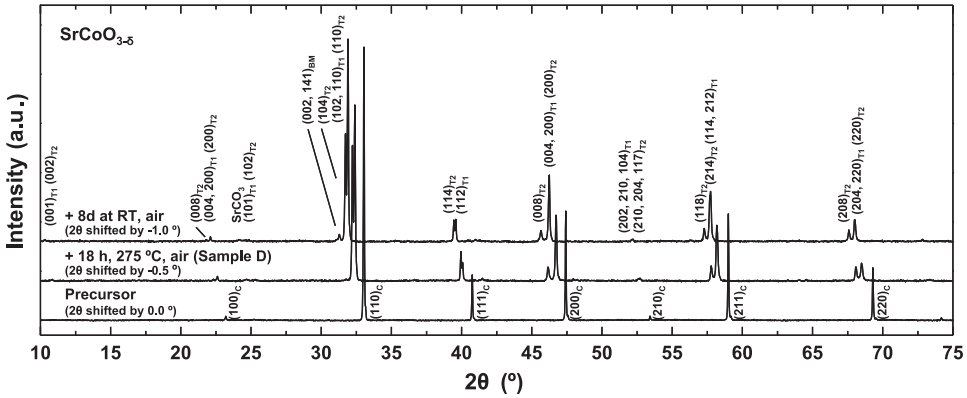

Fig. 1. X-ray diffraction patterns for the precursor $SrCoO_{3-\delta}$ phase (indexed using a cubic unit cell and $pm\bar{3}m$ space group) and the multi-phase Sample D (indexed using two tetragonal $SrCoO_{3-\delta}$ unit cells, T1: $a_C \times a_C \times 2a_C$ and T2: $a_C \times a_C \times 4a_C$, and $I4/mmm$ space group) recorded right after the annealing treatment and after 8 days of standing in air at room temperature. (*Note*: In order to observe the overlapping reflections, the latter two patterns are shifted with respect to their original 2θ scale.)

Table 1
Annealing conditions and the resultant chemical compositions together with lattice parameters and mutual phase ratios determined for the two tetragonal phases (T1 and T2) in the four $SrCoO_{3-\delta}$ multi-phase samples air-annealed for reduction.

	Air-annealing conditions	Chemical composition	Lattice parameters (Å)		Phase ratio: T2/(T1 + T2)[a] (%)
			T1	T2	
Sample A	200 °C, 18 h	$Sr_{0.96(1)}CoO_{2.72(1)}$	$a_{T1} = 3.843(1)$ $c_{T1} = 7.696(1)$	$a_{T2} = 3.840(1)$ $c_{T2} = 15.5571)$	9
Sample B	250 °C, 12 h	$Sr_{0.97(1)}CoO_{2.69(1)}$	$a_{T1} = 3.843(1)$ $c_{T1} = 7.696(1)$	$a_{T2} = 3.840(1)$ $c_{T2} = 15.555(1)$	35
Sample C	250 °C, 18 h	$Sr_{0.97(1)}CoO_{2.68(1)}$	$a_{T1} = 3.843(1)$ $c_{T1} = 7.697(1)$	$a_{T2} = 3.840(1)$ $c_{T2} = 15.553(1)$	44
Sample D	275 °C, 18 h	$Sr_{0.96(1)}CoO_{2.67(1)}$	$a_{T1} = 3.843(1)$ $c_{T1} = 7.697(1)$	$a_{T2} = 3.840(1)$ $c_{T2} = 15.548(1)$	58

[a] Estimated using the integrated intensities of Gaussians fitted under the pseudocubic $(1\,1\,1)_C$ reflections.

accordance with the stabilization of the sample weight in an isothermal TG run at 250 °C in air (Fig. 2(a), upper panel). More interestingly, cooling the sample below $T = 150$ °C results in a split of the $(1\,1\,1)_C$ reflection (Fig. 2(b)), which becomes gradually more prominent with decreasing temperature. The splitting behavior shows reversibility so that the two split reflections merge again at $T > 150$ °C.

As demonstrated in Fig. 1 for Sample D, all the ex situ XRD patterns for the air-reduced samples are characterized by doubled pseudo-cubic reflections. Sample D also demonstrates the instability of the reduced samples at room temperature in air: some of the more intensive characteristic reflections from the orthorhombic BM-type (*Imma*) $SrCoO_{2.5}$ phase [8,16] can be seen already after 8 days of aging at RT. The sluggish decomposition into BM is accompanied with a redistribution of intensities of the doubled pseudo-cubic reflections: the lower-angle reflection of each reflection pair loses intensity in favor of the higher-angle reflection.

Fig. 3(a) and (b) illustrates, respectively, the pseudocubic $(1\,1\,1)_C$ and $(2\,1\,1)_C$ reflections recorded for the four air-annealed samples. In Sample A with $(3-\delta)_{aver} = 2.72(1)$, the lower-angle reflections are almost nonexistent, whereas the Samples B–D show various intensity distributions. As a general rule, the longer the

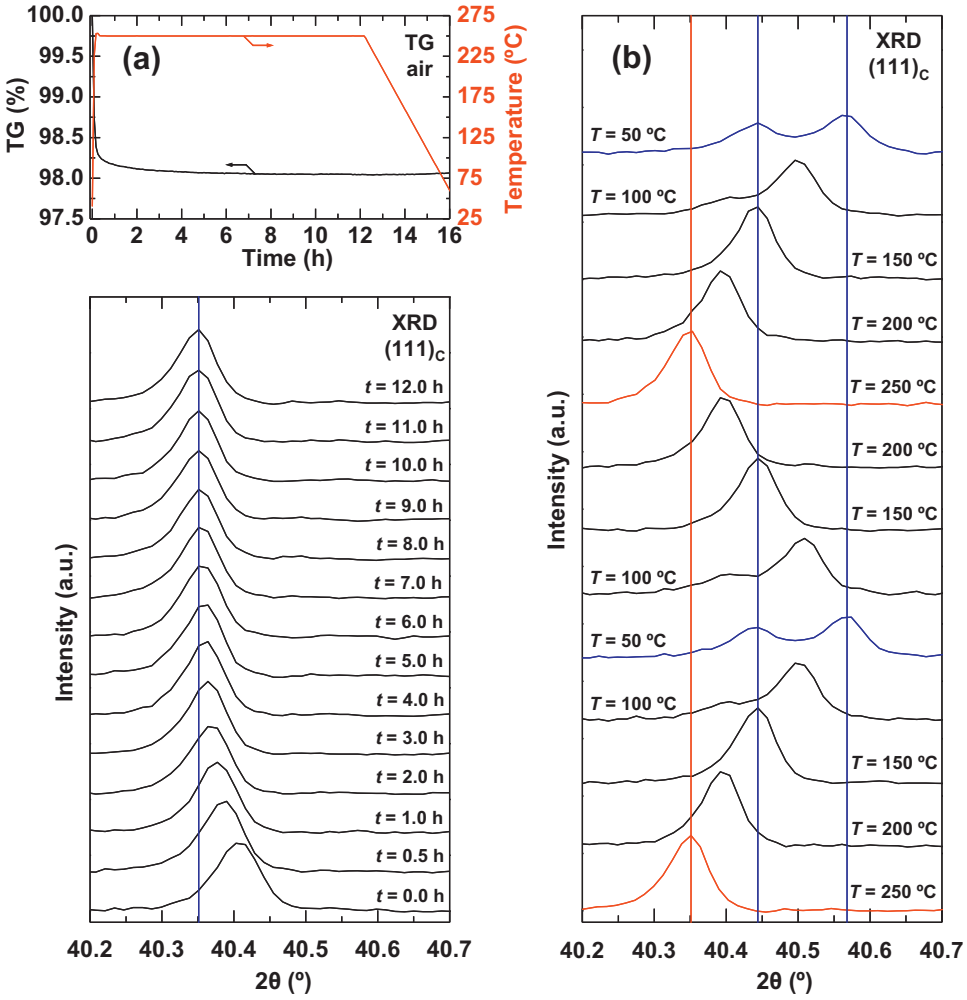

Fig. 2. (a) Oxygen deintercalation from $SrCoO_{3-\delta}$ precursor phase (at 250 °C, 1 atm stagnant air) as seen through weight reduction in TG analysis (upper panel) and negative 2θ shift in in situ XRD patterns (lower panel). (b) Split of the pseudocubic $(1\,1\,1)_C$ reflection at $T < 150$ °C due to the separation of the two tetragonal phases T1 and T2.

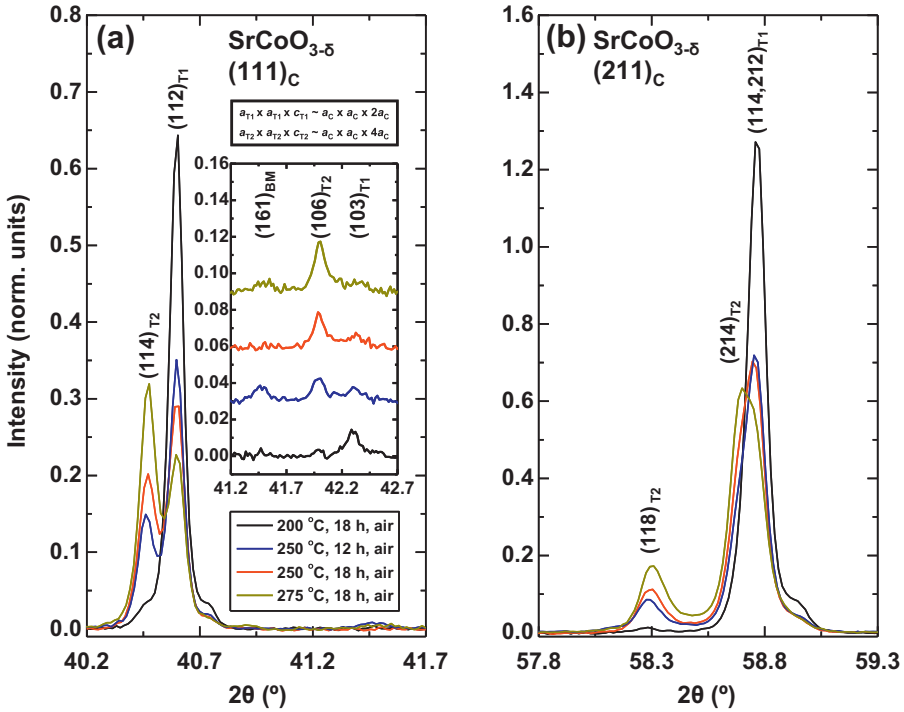

Fig. 3. Pseudocubic (a) $(1\,1\,1)_C$ and (b) $(2\,1\,1)_C$ reflections of oxygen-deintercalated $SrCoO_{3-\delta}$ samples demonstrating the existence of two tetragonal phases, T1 and T2. (*Note*: The weak shoulders at 40.8° and 59.0° originate from the unfiltered part of the Cu-$K_{\alpha 2}$ radiation.)

annealing time and/or the higher the annealing temperature is, the more intensified the lower-angle reflections are. It is interesting, however, that all of Samples B–D have roughly the same $(3-\delta)_{aver}$ value around 2.68(1) (see Table 1).

Different unit cells were attempted in order to index the reflections not related to the BM phase. Eventually, two phases of tetragonal unit cells (named from now on as T1 and T2) were found as satisfactory solutions. Indexation is demonstrated in Fig. 1 for Sample D. The conclusion was based on the following two observations. Firstly, the 2θ positions of the overlapping $(2\,1\,1)_C$ reflections between 58.5° and 59.1° (Fig. 3(b)) stay nearly fixed, implying phase separation rather than a change in lattice distortion, which is expected to show mutually drifting 2θ positions. Secondly, clear difficulties were faced when attempts were made to fit the pseudocubic $(1\,1\,1)_C$ (Fig. 3(a)) and $(2\,1\,1)_C$ (Fig. 3(b)) reflections with a single unit cell.

The observed superlattice reflections (see *e.g.* Fig. 3(a), inset) indicated, respectively, $a_C \times a_C \times 2a_C$, and $a_C \times a_C \times 4a_C$ unit-cell dimensions (a_C = pseudo-cubic lattice parameter) for phases T1 and T2. The given superlattice dimensions with a space group $I4/mmm$ are adequate to yield the reflection positions. Yet it needs to be noted that the actual superlattice and its symmetry depend on the oxygen ordering and may be larger than the one used here. Lattice parameters for the two phases, T1 and T2 (as determined for each of the samples) are summarized in Table 1. The a parameters of the two phases are very close such that a_{T1} is only 0.05% longer than a_{T2}. On the other hand, while T1 has only a minor distortion from cubic symmetry with 0.16% elongation of the c_{T1} parameter from the ideal cubic value (as compared with a_{T1} parameter), T2 has a much stronger tetragonal distortion with 1.23 ... 1.30% of relative c_{T2} elongation. Phase T2 also contrasts to T1 with its evolving c_{T2} parameter, which shows contraction with increasing phase abundancy of T2 (Table 1). The difference in the behavior of the c_{T2} parameter is directly visible in the shifting of the pseudocubic $(2\,0\,0)_C$ reflection pair (Fig. 4): the lower-angle reflection is particular to phase T2, the d value corresponding to the distance

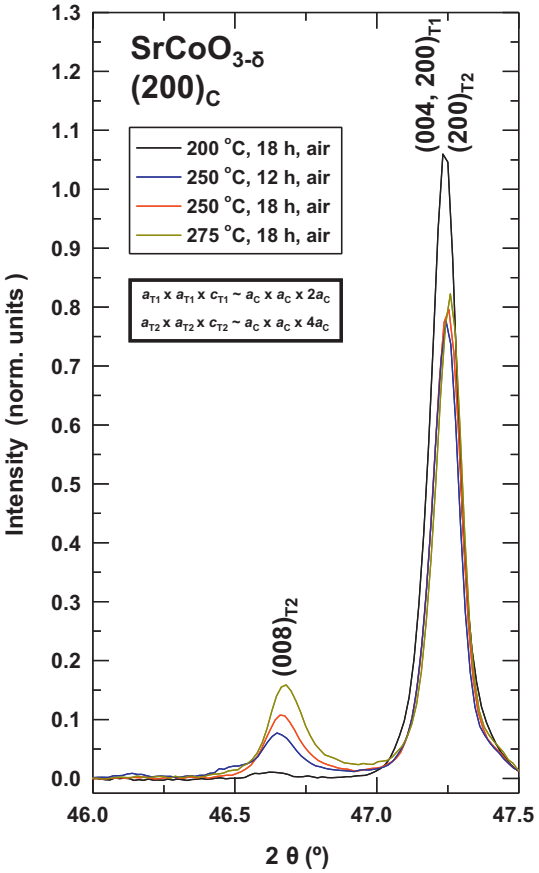

Fig. 4. Pseudocubic $(2\,0\,0)_C$ reflections of oxygen-deintercalated $SrCoO_{3-\delta}$ samples demonstrating the pronounced contraction of the c_{T2} lattice parameter following the increasing abundancy of phase T2.

between the $(0\,0\,2)_C = (0\,0\,8)_{T2}$ planes. The higher-angle reflection, on the other hand, consists of reflections from both phases, T1 and T2, with d values corresponding to the $(2\,0\,0)_C = (2\,0\,0)_{T1,T2}$, $(0\,2\,0)_C = (0\,2\,0)_{T1,T2}$ and $(0\,0\,2)_C = (0\,0\,4)_{T1}$ plane distances. The lower-angle reflection (affected by the c_{T2} parameter) presents a stronger shift than the higher-angle reflection (unaffected by c_{T2}).

4. Discussion

Including the BM phase, appearing as a result of sample aging, three phases were observed in the oxygen-content range $2.50 < (3-\delta)_{aver} < 2.75$. The unchanged lattice-parameter values revealed for the T1 phase suggest a single value of $(3-\delta)_{T1}$. As T1 gets more abundant towards $(3-\delta)_{aver} = 2.75$, we tend to believe (despite the 3% A-site cation deficiency present in T1) that this phase represents the $SrCoO_{2.75}$ stoichiometry (or the $n = 4$ member in the $SrCoO_{(3n-1)/n}$ series), frequently encountered as a relatively stable single phase in oxygen-deficient perovskite systems [8,23–25]. However, while T1 gives a tetragonal XRD pattern, previously reported crystal structure analyses for $SrCoO_{2.75}$ [7,8] concluded a primitive cubic symmetry. A minute tetragonal c_{T1}-axis elongation becomes apparent only through the weak superlattice reflections. If the profile fitting is performed assuming cubic symmetry, the pseudocubic lattice parameter $a_C = 3.843(1)$ Å corresponds to the values reported previously [7,8]. We tentatively suggest that the low-temperature annealing route employed here stabilizes the long-range ordering better than the room-temperature electrochemical techniques used in previous works [7,8].

In the case of phase T2, the slight variation in the c_{T2} parameter suggests some flexibility in the oxygen content for this phase, which is consistent with the fact that the T2/(T1 + T2) phase ratio seems to vary within constant $(3-\delta)_{aver} = 2.68(1)$ value (Table 1). Moreover, the observable contraction only in the c-axis direction of the T2 phase with increasing T2/(T1 + T2) (Table 1) indicates a layered oxygen-vacancy-ordered structure as in the BM phase [15]. Finally, the flexibility of the $(3-\delta)_{T2}$ value coupled with c_{T2} contraction while increasing T2/(T1 + T2) suggest the phase transition from the oxygen-rich T1 phase to the oxygen-poor T2 phase occurs in two steps, as described in Eqs. (1) and (2)

$$SrCoO_{2.75} \rightarrow (1-y)SrCoO_{2.75} + ySrCoO_{2.68+z(\min)} + y(0.035 - 0.5z)O_2 \quad (1)$$

where $y \leq 0.07/[0.07 - z(\min)]$ and $z(\min) \leq 0$.

$$(1-y)SrCoO_{2.75} + ySrCoO_{2.68+z} \rightarrow SrCoO_{2.68} \quad (2)$$

where $y = 0.07/[0.07 - z]$ and $z(\min) \leq z \leq 0$.

In the first step (Eq. (1)) the $(3-\delta)_{aver}$ changes from 2.75 to 2.68. The T2 phase segregating from the T1 phase presents the minimum value for $(3-\delta)_{T2} = 2.68 + z(\min)$. The second step (Eq. (2)) then initiates after reaching $(3-\delta)_{aver} = 2.68$. Here the T2 phase formation is accompanied by $(3-\delta)_{T2} = 2.68 + z$ elevation until the single phase with $(3-\delta)_{T2} = 2.68$ is reached.

The suggested $(3-\delta)_{T1} = 2.75$ and $(3-\delta)_{T2} = 2.68$ stoichiometries closely correspond to those of the $n = 4$ and $n = 3$ members in the $SrCoO_{(3n-1)/n}$ ($Sr_nCo_nO_{3n-1}$) homologous series, typical for the oxygen-deficient $ABO_{3-\delta}$ perovskites [26,27]. While numerous examples exist for the $A_2B_2O_5$ ($n = 2$), $A_4B_4O_{11}$ ($n = 4$) and $A_8B_8O_{23}$ ($n = 8$) stoichiometries [8,16,23–25,28,29], phases with the $A_3B_3O_8$ ($n = 3$) stoichiometry are rare. To our knowledge $La_3Co_3O_8$ ($P2_1$) [30], $La_3Ni_3O_8$ (unit-cell symmetry unknown) [31] and $La_3Cu_3O_8$ ($P2/m$) [32,33] stand as the only examples of the $n = 3$ homologues up to date. It should be mentioned that much more examples of the $n = 3$ type stoichiometry exist among the substituted perovskites, such as in the $Ca_{3-x}A_xFe_{3-y}B_yO_8$ (A = Sr, Ba, Y, La, Gd; B = Ti) (orthorhombic) [26,34] system. A further example is the $Sr_{1-x}(Y,Ln)_xCoO_{3-\delta}$ (Ln = Sm, Gd, Dy, Ho, Er, Tm, Yb; $x \leq 0.33$) system. Some of its members show either tetragonal ($I4/mmm$) or orthorhombic ($Cmma$) single phases within $0.25 < \delta < 0.50$ [35–37]. The results given here strongly indicate that the $Sr_3Co_3O_8$ (*i.e.* $SrCoO_{2.67}$) stoichiometry also exists as a long-range ordered structure. With its tetragonal unit cell, T2 appears to have an exceptionally high symmetry for an $n = 3$ homologue, as compared with the so far synthesized non-substituted phases typically presenting monoclinic unit cells [30–33].

5. Conclusions

Topotactic oxygen deintercalation was realized in the $SrCoO_{3-\delta}$ system by using a simple set-up based on atmospheric-pressure annealing of cubic oxygen-rich $SrCoO_{3-\delta}$ perovskite in air. The annealing temperatures were unusually low for oxide materials, in accordance with the relatively high low-temperature oxygen mobility in the $SrCoO_{3-\delta}$ system.

Within the $0.25 < \delta < 0.50$ region, three phases were detected: two tetragonal phases (T1 and T2) and the brownmillerite $SrCoO_{2.5}$. Phase T1 was concluded to be $SrCoO_{2.75}$; a very weak tetragonal distortion along the c-axis was detected for the T1. Phase T2, on the other hand, possesses a new layered structure with a strong tetragonal c-axis elongation. As phase T2 experiences a sluggish decomposition into BM and T1, it is understood to be an intermediate phase between the relatively stable $n = 2$ ($SrCoO_{2.5}$) and $n = 4$ ($SrCoO_{2.75}$) phases and therefore to be the missing member $n = 3$ of the $SrCoO_{(3n-1)/n}$ homologous series.

More elaborated methods, such as neutron powder diffraction, are necessary to clarify the oxygen ordering scheme. High-resolution synchrotron XRD data are also needed for concluding the true unit-cell dimensions and the eventual symmetry of the T2 phase. Furthermore, the possibility of twinning-induced nanodomain structures at $T < 150$ °C, as presented by the $0.58 < \delta < 0.71$ region reported earlier, should be investigated using HRTEM and ED. In order to proceed into this direction, the stabilization of T2 within a single phase sample needs to be achieved.

Acknowledgements

The present work was supported by Academy of Finland (Nos. 126528 and 130352), Tekes (No. 1726/31/07) and the Finnish Foundation for Technology Promotion.

References

[1] A. Nemudry, P. Rudolf, R. Schöllhorn, Solid State Ionics 109 (1998) 213.
[2] S. Bhavaraju, J.F. DiCarlo, D.P. Scarfe, A.J. Jacobson, D.J. Buttrey, Solid State Ionics 86–88 (1996) 825.
[3] P. Rudolf, R. Schöllhorn, J. Chem. Soc., Chem. Commun. (1992) 1158.
[4] A. Nemudry, M. Weiss, I. Gainutdinov, V. Boldyrev, R. Schöllhorn, Chem. Mater. 10 (1998) 2403.
[5] Y. Tsujimoto, C. Tassel, N. Hayashi, T. Watanabe, H. Kageyama, K. Yoshimura, M. Takano, M. Ceretti, C. Ritter, W. Paulus, Nature 450 (2007) 1062.
[6] P. Bezdicka, A. Wattiaux, J.C. Grenier, M. Pouchard, P. Hagenmuller, Z. Anorg. Allg. Chem. 619 (1993) 7.
[7] A. Nemudry, P. Rudolf, R. Schöllhorn, Chem. Mater. 8 (1996) 2232.
[8] R. Le Toquin, W. Paulus, A. Cousson, C. Prestipino, C. Lamberti, J. Am. Chem. Soc. 128 (2006) 13161.
[9] L. Karvonen, S. Räsänen, H. Yamauchi, M. Karppinen, Chem. Lett. 36 (2007) 1176.
[10] L. Karvonen, H. Yamauchi, M. Karppinen, Chem. Mater. 20 (2008) 7143.
[11] L. Karvonen, M. Valkeapää, R.S. Liu, J.M. Chen, H. Yamauchi, M. Karppinen, Chem. Mater. 22 (2010) 70.
[12] S. Räsänen, H. Yamauchi, M. Karppinen, Chem. Lett. 37 (2008) 638.
[13] M. Trari, J. Töpfer, J.P. Doumerc, M. Pouchard, A. Ammar, P. Hagenmuller, J. Solid State Chem. 111 (1994) 104.
[14] D.G. Hinks, O. Chmaissem, L. Ely, C. Scott, J.D. Jorgensen, J.K. Akujieze, Physica C 333 (2000) 1.
[15] Y. Takeda, R. Kanno, T. Takada, O. Yamamoto, M. Takano, Y. Bando, Z. Anorg. Allg. Chem. 540/541 (1986) 259.

[16] J.C. Grenier, S. Ghodbane, G. Demazeau, M. Pouchard, P. Hagenmuller, Mater. Res. Bull. 14 (1979) 831.
[17] S. Stemmer, A. Sane, N.D. Browning, T.J. Mazanec, Solid State Ionics 130 (2000) 71.
[18] V.V. Vashook, M.V. Zinkevich, Yu.G. Zonov, Solid State Ionics 116 (1999) 129.
[19] P.E. Werner, L. Eriksson, M. Westdahl, J. Appl. Crystallogr. 18 (1985) 367.
[20] V. Petricek, M. Dusek, The Crystallographic Computing System JANA2000, Institute of Physics, Praha, Czech Republic, 2000.
[21] L. Bedel, A.C. Roger, C. Estournes, A. Kiennemann, Catal. Today 85 (2003) 207.
[22] D. Waller, J.A. Lane, J.A. Kilner, B.C.H. Steele, Mater. Lett. 27 (1996) 225.
[23] N.N. Loshkareva, N.V. Mushnikov, A.V. Korolyov, E.A. Neifeld, A.M. Balbashov, Phys. Rev. B 77 (2008) 052406.
[24] J.P. Hodges, S. Short, J.D. Jorgensen, X. Xiong, B. Dabrowski, S.M. Mini, C.W. Kimball, J. Solid State Chem. 151 (2000) 190.
[25] J.M. González-Calbet, M.J. Sayagués, M. Vallet-Regí, Solid State Ionics 32–33 (1989) 721.
[26] J.C. Grenier, J. Darriet, M. Pouchard, P. Hagenmuller, Mater. Res. Bull. 11 (1976) 1219.
[27] S. Stølen, E. Bakken, C.E. Mohn, Phys. Chem. Chem. Phys. 8 (2006) 429.
[28] V. Caignaert, N. Nguyen, M. Hervieu, B. Raveau, Mater. Res. Bull. 20 (1985) 479.
[29] T. Moriga, M. Hayashi, T. Sakamoto, M. Orihara, I. Nakabayashi, Solid State Ionics 154–155 (2002) 251.
[30] O.H. Hansteen, H. Fjellvåg, B.C. Hauback, J. Mater. Chem. 8 (1998) 2081.
[31] T. Moriga, O. Usaka, I. Nagabayashi, T. Kinouchi, S. Kikkawa, F. Kanamaru, Solid State Ionics 79 (1995) 252.
[32] S.J. La Placa, J.F. Bringley, B.A. Scott, D.E. Cox, J. Solid State Chem. 118 (1995) 170.
[33] M. Karppinen, H. Yamauchi, H. Suematsu, K. Isawa, M. Nagano, R. Itti, O. Fukunaga, J. Solid State Chem. 130 (1997) 213.
[34] J.C. Grenier, F. Ménil, M. Pouchard, P. Hagenmuller, Mater. Res. Bull. 12 (1977) 79.
[35] S.Ya. Istomin, J. Grins, G. Svensson, O.A. Drozhzhin, V.I. Kozhevnikov, E.V. Antipov, J.P. Attfield, Chem. Mater. 15 (2003) 4012.
[36] A. Maignan, S. Hébert, V. Caignaert, V. Pralong, D. Pelloquin, J. Solid State Chem. 178 (2005) 868.
[37] M. James, M. Avdeev, P. Barnes, L. Morales, K. Wallwork, R. Withers, J. Solid State Chem. 180 (2007) 2233.